

Review

Are Clay Minerals Systematically the Products of Aqueous Alteration in Cosmic Bodies?

Abderrazak El Albani ^{1,*}, Ibtissam Chraiki ^{1,*}, Hasnaa Chennaoui Aoudjehane ², Mohamed Ghnahalla ¹, Fatima Abdelfadel ³, Ahmed Abd Elmola ⁴, Olabode Bankole ¹, Julie Ngwal'ghoubou Ikouanga ¹, Anna El Khoury ^{1,5}, Claude Fontaine ¹, El Hafid Bouougri ⁶, France Westall ⁷ and Alain Meunier ¹

¹ Institut de Chimie des Milieux et Matériaux, Université de Poitiers and CNRS, 86073 Poitiers, France; mohamed.ghnahalla@univ-poitiers.fr (M.G.); boardgeo@yahoo.com (O.B.); ngwaljulie@gmail.com (J.N.I.); anna.el.khoury@univ-poitiers.fr (A.E.K.); claude.fontaine@univ-poitiers.fr (C.F.); alain.meunier@univ-poitiers.fr (A.M.)

² GAIA Laboratory, Faculty of Sciences Ain Chock, Hassan II University of Casablanca, km 8 Route d'El Jadida, Casablanca 20150, Morocco; chennaoui_h@yahoo.fr

³ National Institute for Scientific and Technological Research in Water, City of Innovation Souss Massa, Ibn Zohr University, Agadir 80000, Morocco; f.abdelfadel@gmail.com

⁴ The James Hutton Institute, Craigiebuckler, Aberdeen AB15 8QH, UK; abd_elmola.ahmed@yahoo.com

⁵ Nanoscopium Beamline, Synchrotron Soleil, 91192 Gif-sur-Yvette, France

⁶ Department of Geology, Faculty of Sciences-Semlalia, Cadi Ayyad University, Marrakesh 40000, Morocco; bouougri@uca.ma

⁷ CNRS-Centre de Biophysique Moléculaire, 45100 Orléans, France; frances.westall@cnrs.fr

* Correspondence: abder.albani@univ-poitiers.fr (A.E.A.); ibtissamchraiki@gmail.com (I.C.)

Abstract: The formation of chondrite materials represents one of the earliest mineralogical processes in the solar system. Phyllosilicates are encountered at various stages of the chondrule formation, from the initial stages (IDP agglomerates) to the final steps (chondrule internal alteration). While typically linked to aqueous alteration, recent studies reveal that phyllosilicates could precipitate directly from residual fluids in post-magmatic or deuteric conditions and under a wide range of temperatures, pressures, water/rock ratios, and H₂/H₂O ratio conditions. This study re-examined the formation of hydrated phyllosilicates in chondrules and associated fine-grained rims (FGRs) using published petrographical, mineralogical, and chemical data on carbonaceous chondrites. Given that chondrules originate from the melting of interplanetary dust particles, the water liberated by the devolatilization of primary phyllosilicates, including clay minerals or ice melting, reduces the melting temperature and leads to water dissolution into the silicate melt. Anhydrous minerals (e.g., olivine and diopside) form first, while volatile and incompatible components are concentrated in the residual liquid, diffusing into the matrix and forming less porous FGRs. Serpentine and cronstedtite are the products of thermal metamorphic-like mineral reactions. The mesostasis in some lobated chondrules is composed of anhydrous and hydrous minerals, i.e., diopside and serpentine. The latter is probably not the alteration product of a glassy precursor but rather a symplectite component (concomitant crystallization of diopside and serpentine). If so, the symplectite has been formed at the end of the cooling process (eutectic-like petrographical features). Water trapped inside chondrule porosity can lead to the local replacement of olivine by serpentine without external water input (auto-alteration). In the absence of water, hydrated phyllosilicates do not crystallize, forming a different mineral assemblage.

Keywords: cosmic bodies; clay minerals; meteorites; chondrite; phyllosilicates; aqueous alteration



Citation: El Albani, A.; Chraiki, I.; Aoudjehane, H.C.; Ghnahalla, M.; Abdelfadel, F.; Elmola, A.A.; Bankole, O.; Ikouanga, J.N.; El Khoury, A.; Fontaine, C.; et al. Are Clay Minerals Systematically the Products of Aqueous Alteration in Cosmic Bodies? *Minerals* **2024**, *14*, 486. <https://doi.org/10.3390/min14050486>

Academic Editor: Yasuhiro Sekine

Received: 5 April 2024

Revised: 30 April 2024

Accepted: 1 May 2024

Published: 3 May 2024



Copyright: © 2024 by the authors. Licensee MDPI, Basel, Switzerland. This article is an open access article distributed under the terms and conditions of the Creative Commons Attribution (CC BY) license (<https://creativecommons.org/licenses/by/4.0/>).

1. Introduction

Chondrites are mechanical mixtures of a variety of components, each of which originated from distinct periods and regions within the protosolar nebula. They encompass

grains predating the solar nebula's formation, known as presolar grains, varying in prevalence across specimens [1]. The proportions and sizes of the main chondritic constituents serve as crucial classifiers for meteorites. These constituents include chondrules, FeNi metals, refractory inclusions like Ca–Al-rich inclusions (CAIs) and amoeboid olivine aggregates (AOAs), fine-grained matrix, and presolar grains [2].

The term “carbonaceous chondrites” refers to a class of meteorites that was initially composed of three groups, connected by relatively high carbon and water abundances [3]. Currently, nevertheless, the class consists of eight distinct compositional groups of CI, CM, CR, CO, CV, CK, CH, and CB chondrites [4], the majority of which are not notably richer in water or carbon [5]. They are now collectively grouped based on their largely unfractionated bulk chemical composition relative to that of the sun [4]. It is currently assumed that these individual groups are not genetically related and likely do not originate from the same parent object [1]. Among these groups, CI chondrites are the most primitive, displaying a composition nearly identical to that of the solar photosphere for all but the most volatile elements [6,7].

The mineralogy of carbonaceous chondrites remains relatively consistent across groups, comprising varying proportions of olivine, pyroxene, plagioclase, phyllosilicates, organic matter, and presolar grains [1,2]. These minerals are distributed among the different components within the chondrites, such as chondrules, Cals, and matrix [1,2]. High-temperature processes during the collapse of the presolar nebula, exceeding 1500 °C, formed calcium-aluminum-rich inclusions (CAIs) and chondrules [1]. Conversely, in other phases, such as the matrix formed through lower-temperature processes occurring after material aggregation into parent bodies [1], hydrated phyllosilicates are common in different carbonaceous chondrites, especially in the matrix of CI and CM types. Their presence, specifically clay minerals, in meteorites has been known for decades [8,9]. They are considered to be the alteration products of pre-existing glass, amorphous silicates, olivine, and pyroxene [9–12], or metal grains [9]. Liquid water was supplied by the melting of water ice by the heat flux generated either by decaying short-living radionuclides, such as ²⁶Al and ⁶⁰Fe [13–15], or locally by shocks between asteroidal bodies [16,17]. The duration of heat dissipation in asteroidal bodies may be sufficient to maintain water in the liquid state for a long period of time, enough to trigger alteration processes [18].

The most commonly encountered phyllosilicates in carbonaceous chondrites include Fe, Mg-rich species of smectites (saponite, nontronite), serpentine, and cronstedtite [19,20]. They have been identified in the matrix as well as in the chondrules and associated fine-grained rims (FGRs). Similar clay minerals are observed in terrestrial basalts, resulting from alteration processes involving water, either externally (e.g., seawater) or internally (e.g., olivine iddingsitization), interacting with glassy basaltic rock [21]. Additionally, clay minerals can precipitate directly from residual magmatic fluid at the end of the cooling stage of basaltic lavas [21,22]. The exploration of diverse formation processes for Fe- and Mg-rich phyllosilicates on earth, as highlighted in the preceding paragraph, underlines the necessity to re-evaluate established assumptions regarding their origins in chondrites. This is crucial for advancing our understanding of the early solar system, elucidating the distribution and history of water, and the processes that have shaped planetary bodies throughout their history. In line with this, the present paper seeks to elucidate the characteristic features of aqueous alteration and reassess the mechanisms underlying the formation of clay minerals in specific meteorites. By reinterpreting published data through the lens of terrestrial processes, this study aims to contribute to a deeper understanding of the complexities surrounding alteration processes in meteoritic materials.

2. Results and Discussion

2.1. Terrestrial Alteration Processes

Alteration processes are ubiquitous across Earth's diverse landscapes, manifesting from surface environments to deep zones within volcanic areas such as hydrothermal fields, as well as in sedimentary basins (diagenetic processes) and in fractured rocks. This alter-

ation results from water-rock interactions, driven by potential chemical gradients between solutions and primary minerals [23]. The nature and extent of secondary products, mostly clay minerals, depend on two main factors: the magnitude of these gradients and the duration for which they are sustained. In all water–mineral reactions, whether occurring on the Earth’s surface or deep within the crust, they take place within interconnected micro-sites, facilitating chemical exchanges and transformations between water molecules and mineral surfaces [24]. When these micro-sites are well-connected, they behave as thermodynamically open micro-systems, with a constant renewal of fluid. Conversely, poorly connected micro-sites resemble nearly closed micro-systems with resident fluid. The water–mineral reactions trigger the migration of the most soluble chemical components, while the less soluble ones are progressively concentrated in the remaining secondary products.

In open systems, secondary minerals form in place within parent crystals before eventually being destabilized if the solutions are continuously renewed. In such cases, an alteration front is sometimes visible within the rock. In contrast, nearly closed systems feature resident fluids that approach chemical equilibrium with the primary minerals, leading to the formation of polyphase secondary mineral assemblages with bulk chemical compositions closely resembling those of their parent minerals [24].

The chemical transfers and their subsequent mineral reactions not only modify the mineralogical composition of the rock but also change its texture. Indeed, whatever the temperature conditions, any aqueous alteration induces the dissolution of the primary minerals, marked by retreating surfaces and the formation of a secondary porosity [25]. The dissolution–precipitation mechanism results in spectacular saw-tooth surfaces in amphibole or pyroxene [26,27] or corrosion embayments in feldspars.

During the first alteration stage of mafic and ultramafic rocks, amphibole or pyroxene are partly replaced by secondary phyllosilicates, the crystal growth of which is topotactically controlled [25,28]. The chemical transfers operate at a nanoscale, inducing depolymerization of the silicate chain while simultaneously contributing to the formation of the phyllosilicate structure [25,28]. In this case of alteration, both the texture and chemical composition of secondary products are inherited from the parent crystals. However, the replacement is never perfectly isovolumetric; instead, secondary porosity forms concomitantly with the growth of the alteration products [29]. This is systematically the case even when parent and daughter crystals have similar crystal structures, like the albitization of orthoclase [30]. As dissolution intensity increases, micrometer-sized pores form within the parent crystals, within which randomly oriented particles precipitate [26,31].

Glassy rocks exhibit particular alteration features; an hydrated front separates palagonite from unaltered glass, while nanometer-sized clay particles are randomly disseminated inside the palagonite [32]. Dissolution features may be strikingly evident, as in the above-mentioned case of amphibole or pyroxene, or more challenging to detect, as in the progressive invasion of hydration in glassy basaltic rocks, where the accumulation of titanium oxides outlines the alteration front [22].

To summarize, the most critical characteristic of aqueous alteration is the formation of retreating surfaces inside the unstable mineral or glass. However, embayments are not all due to corrosion. Skeletal crystals exhibit engulfed outer surfaces. They typically form during the rapid cooling of magmatic rocks, and the embayments are filled with a microcrystalline matrix. In this case, the crystals have not been dissolved but instead have not achieved full growth (Figure 1).

High-temperature iddingsite (HTI) is a cryptocrystalline aggregate consisting of orthopyroxene, cristoballite, amorphous silica, maghemite, and hematite [33]. It forms through the deuteric alteration of olivine upon contact with residual liquids generated during the cooling phase of lavas. Typically, plagioclase and pyroxene are unaffected. The magmatic environment becomes oxidative because the H₂O molecules are dissociated at high temperatures and change the partial pressure of oxygen [34]. The oxygen and water partial pressures are too high for Mg-rich olivine crystals to remain stable, leading to their alteration into iddingsite. This alteration forms a rim at their outer surfaces, known as

the retreating surface of Mg-rich olivine (Figure 2). Often, this rim is enclosed by Fe-rich olivine overgrowths, providing evidence that iddingsite is undoubtedly a high-temperature alteration feature of Mg-rich olivine [35]. X-ray diffraction (XRD) has not identified any phyllosilicates forming the rim. However, Clément et al. [36], in their study of HTI covered by fayalite overgrowth, demonstrated that microprobe analyses consistently reveal a deficit in oxide summation, which may be attributed to non-analyzed water by correlating it with a loss on ignition. The authors suggest that HTI is composed of hydroxylated, poorly crystalline phases with a coherent scattering domain size too low to diffract X-rays. The nature of these cryptocrystalline hydroxylated mineral phases can be indirectly determined by recalculating their composition on an 11-oxygen basis with iron in the Fe^{3+} state (Figure 2). The HTI composition is similar to that of Fe-rich smectites (nontronite-like) rather than celadonite, which cannot form because of potassium deficiency in the system.

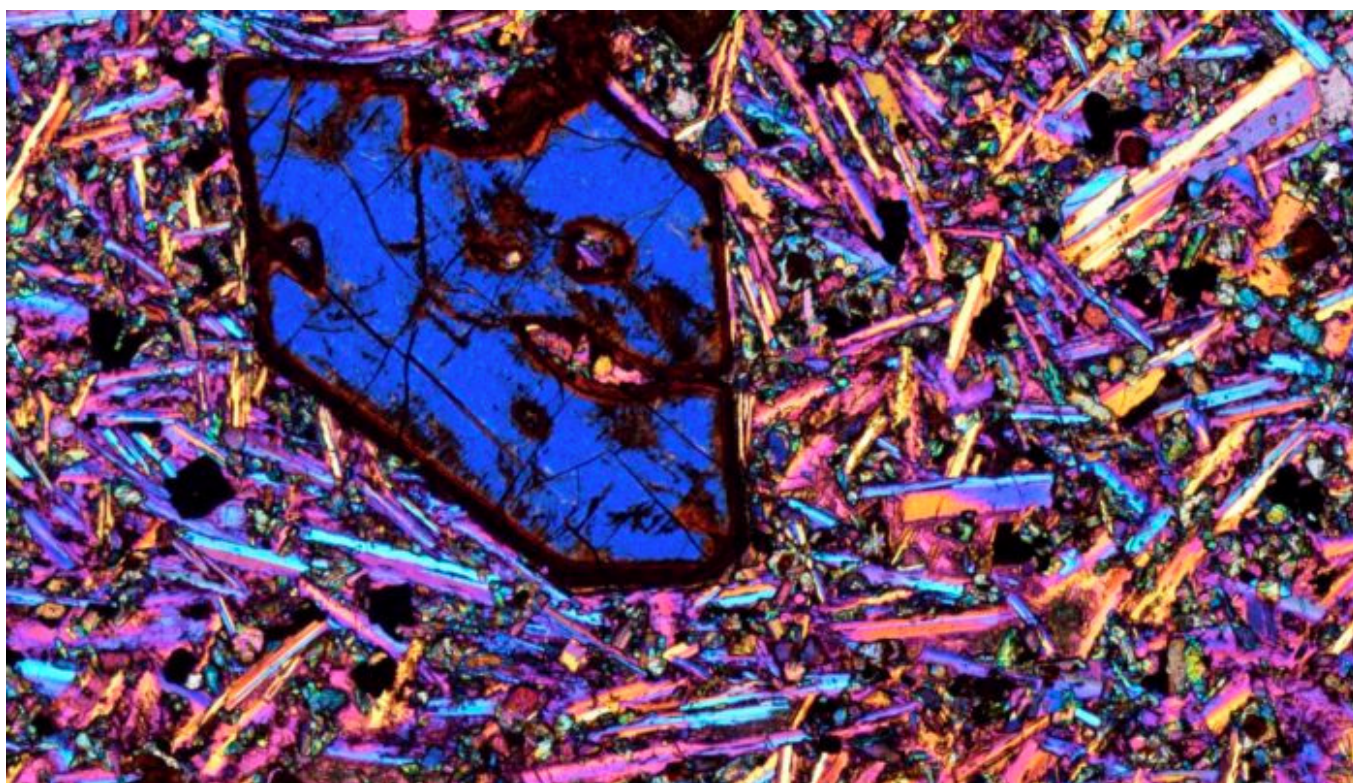


Figure 1. Blue Olivine set in a matrix of pyroxene, magnetite, and plagioclase in a basalt, exhibiting embayments and non-alteration features in basaltic rocks. The embayment observed in the olivine crystal is not associated with alteration; rather, it is attributed to the incomplete growth of the crystal. The sample was collected by the photographer, Bernardo Cesare, on the shore of the Sea of Galilee, Israel. Polarized light photomicrograph. Crossed polarizers and a red tint plate. Width: c. 2.7 mm. EGU creative common license.

In summary, HTI is formed during the last cooling stages [36], and the aqueous source is undoubtedly the residual magmatic liquid. Thus, the physical state of water is probably that of a supercritical fluid. The HTI components, including clay minerals, are auto-alteration products of pyroxene and olivine, which crystallized first.

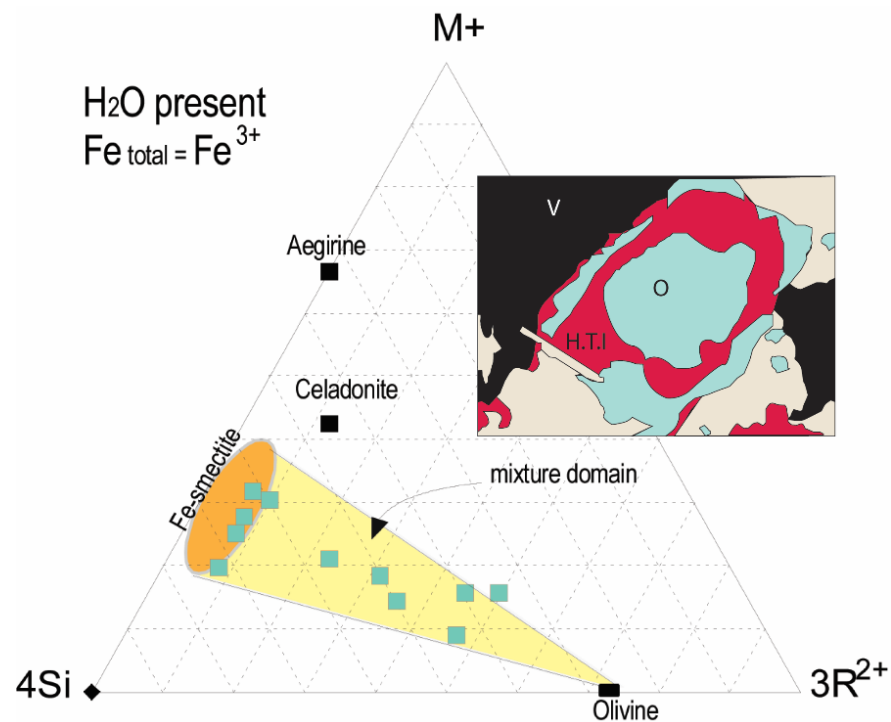


Figure 2. High-temperature iddingsite (HTI). HTI forms a rim around Mg-rich olivine (O.) and is covered by Fe-rich olivine overgrowth (fayalite). V: vesicle. Crossed nicols: 0.63 mm (modified from Figure 1b in [35]). Plotted in the $M^+-4Si-R^{2+}$ diagram [37], the chemical compositions indicate that HTI contains a Fe-rich smectite component (data from [36]). Compositions have been recalculated on an 11-oxygen basis with $Fe = Fe^{3+}$ to be compared with those of iron-rich clay minerals. M^+ : $Na + K + 2Ca$; $4Si$: the number of Si cations divided by 4; $3R^{2+}$: the number of Mg and Mn ions divided by 3.

2.2. Non-Altered Clay Mineral Textures

Clay minerals in basalts, and specifically Fe- and Mg-rich species, are classically thought to form during the diagenesis to low metamorphism stages of volcanic formations [38,39]. Mineral reactions in these environments are initiated by external water inputs. However, since mafic magmas can serve as a source of water [40], similar Fe and Mg clay minerals may also form through non-alteration processes [21]. Upon rapidly reaching the surface, magma often retains a portion of its volatile components due to incomplete degassing. Consequently, lava flows or dikes, sufficiently thick to maintain a molten core between their solidified interfaces with the atmosphere or encasing rocks, tend to concentrate water and other volatile or incompatible components in the residual fluids. These fluids become trapped within the free spaces between magmatic crystals, i.e., the diktytaxitic voids. As temperatures decrease, these fluids become oversaturated with several mineral phases, leading to the co-precipitation of Fe- and Mg-rich clays along with pyroxene, apatite, and K-feldspar (Figure 3a,b). Clay minerals grow on any solid surface according to a geometric selection process [41], forming a palisade-like texture (Figure 3b,c). The crystallization process unfolds in two major steps (Figure 3c): First, clay particles grow in a randomly oriented pattern, enveloping the solid surfaces of minerals regardless of their chemical composition (biotite, K-feldspar, plagioclase, etc.), and reducing the diktytaxitic voids. Subsequently, only the particles oriented toward the center of the void persist in growing, demonstrating a geometric selection process.

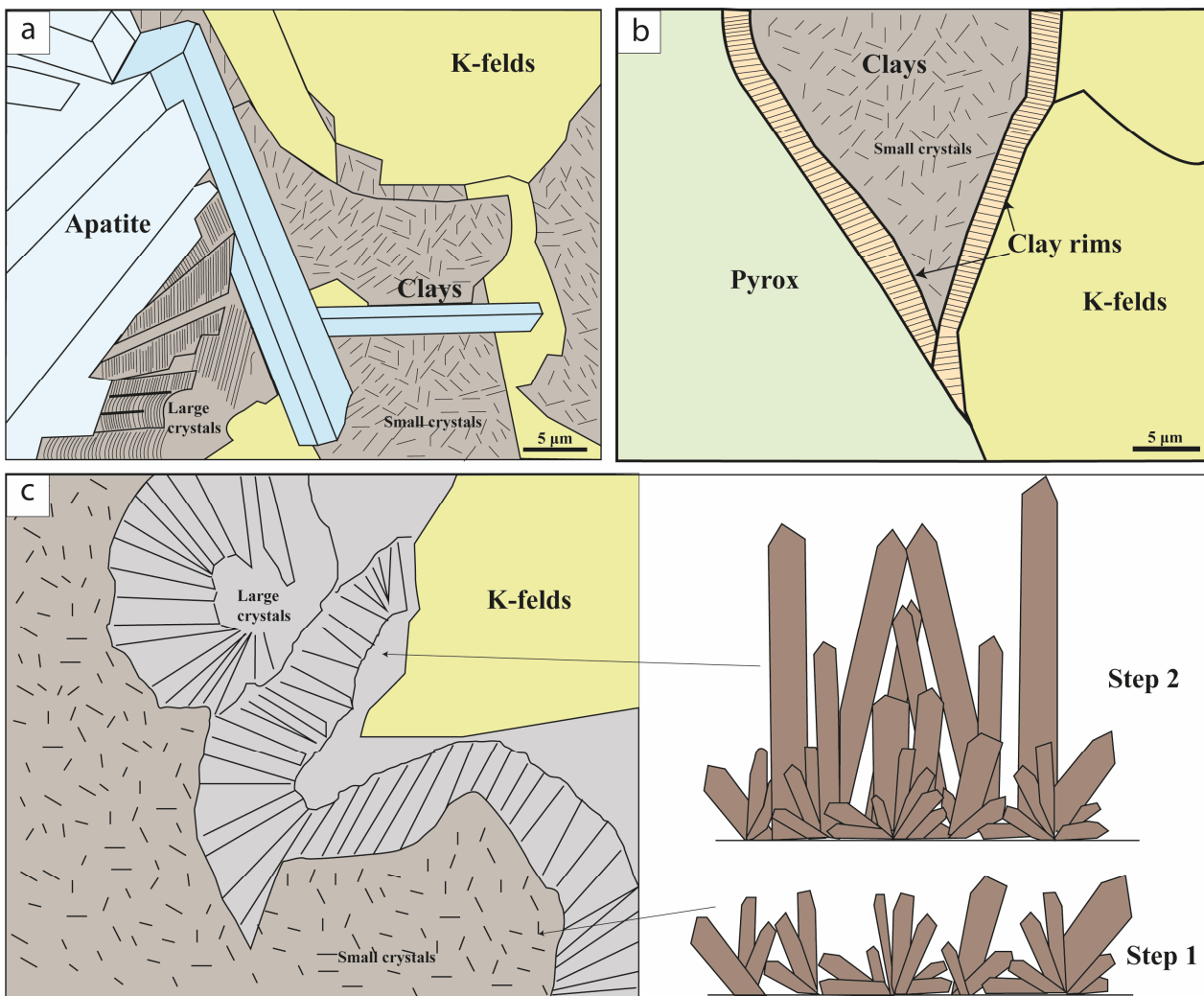


Figure 3. Non-alteration feature in basaltic lava. (a) A reconstruction of a SE image illustrates the direct precipitation of Fe- and Mg-rich clays forming a palissade texture from residual fluid concentrated in free spaces between phenocrysts (dyktytaxitic voids) at the end of the cooling stage. (b) A reconstruction of a SE image showing the pallissadic texture of clay particles forming a regular rim on K-feldspar and pyroxene crystals. (c) The crystal growth of Fe- and Mg-rich clays is controlled by a geometric selection process. Clay particles grow randomly, initially reducing the diktytaxitic voids (small particles, step 1), and then the particles oriented toward the center of the void continue growing to form larger particles (step 2). (a,b) are modified from Figure 3 in [21], and (c) is modified from [42].

The petrographical texture and the enrichment in incompatible elements, such as REE+Y, suggest that the clay minerals do not form by alteration of pre-existing volcanic glass but rather precipitate directly from the residual fluids [21]. Additionally, numerous synthesis experiments of silicates in the presence of water have demonstrated the co-precipitation of anhydrous and hydrated minerals, including clay minerals [43,44]. In summary, Fe and Mg phyllosilicates, which crystallize in nearly closed systems, may be formed by three different processes: (1) alteration in the presence of resident fluids; (2) auto-alteration at the end of the magmatic stage; and (3) direct precipitation from residual fluids. The crystal-chemical properties of these phyllosilicates are not differentiated enough to indicate any one of these processes. Thus, the signatures of alteration, auto-alteration, or direct precipitation from over-saturated fluids need to be looked for at another scale, i.e.,

in the textures of the crystallite assemblages and their petrographical relation with the anhydrous crystals or glass (presence or absence of retreating surfaces).

2.3. Aqueous Alteration in Meteorites

Aqueous alteration refers to the chemical reactions and mineralogical transformations that occur when water interacts with the mineral constituents of carbonaceous chondrites under specific conditions. This alteration process is believed to have occurred in the early stages of the solar system's formation (the first 5 myr) [45], possibly within the parent bodies of these meteorites, such as asteroids or planetesimals [46,47]. These aqueously altered meteorites harbor approximately ≈ 13 wt.% water [48] bound within the structure of phyllosilicates in the form of hydroxyl (HO), such as in serpentine, which are the prevailing mineral phases within these meteorites.

It is assumed that the water flow regime controls aqueous alteration in asteroids. As icy deposits make the outer surface of asteroids impermeable, three different flow regimes are possible [49]: static water, water exhalation (single pass flow), and convection (multiple pass flow) (Figure 4). To explain the fact that the CI chondrites, which have a composition close to that of the Sun's photosphere, are paradoxically the most altered meteorites, Young et al. [49] propose that they originated from asteroids with diameters smaller than 80 km. In such environments, alteration proceeds in an isochemical manner, leading to static water flow as the controlling mechanism for this process (Figure 4).

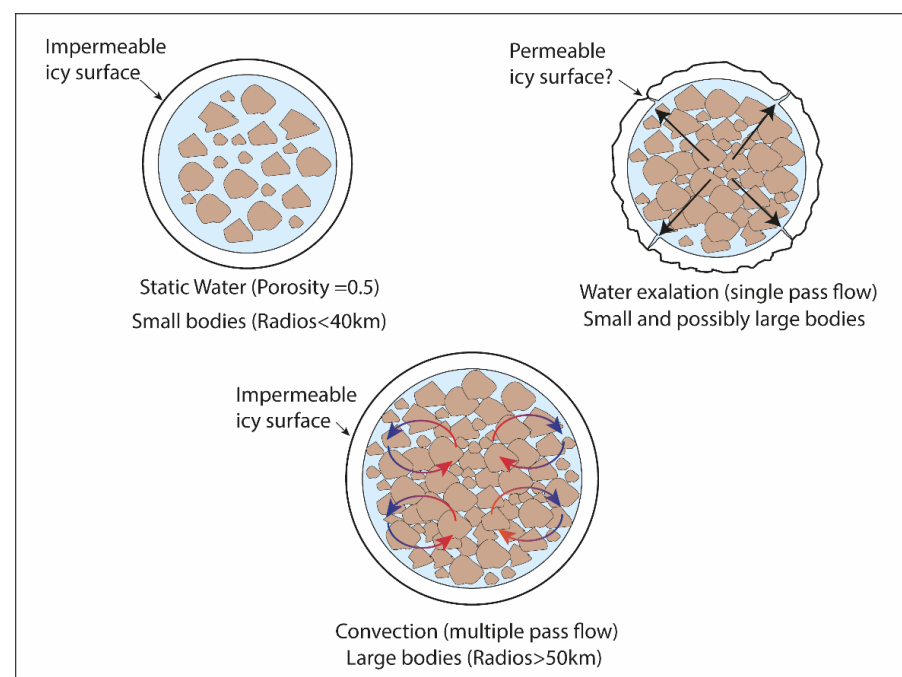


Figure 4. A schematic illustration of the three modes of water rock interaction in asteroid (modified after [49]). The diagram illustrates porosity at a macroscopic scale (in kilometers), while the calculations are conducted using microscopic (grain-scale) porosity for accuracy [49]. Blue represents liquid water, and the tick arrows represent the direction of pore water flow.

The multistage alteration model seems to be the most frequently applied to CI and CM chondrites [50]. However, even with a multistage alteration, its duration is not long enough for water/rock interaction to significantly modify the chondrite's chemical composition. In other words, one may consider that most mineral reactions induced by aqueous alteration occur in closed or nearly closed systems. This was confirmed by Bland et al. [51], who studied the chemical exchanges between chondrules and matrices in different carbonaceous meteorites. These authors suggested that aqueous alteration cannot explain the fractionation of volatile and moderately volatile elements between chondrules and matrix, as well as

the non-monotonic trace element patterns observed in both components. They demonstrate that when evidence of alteration exists, it is predominantly isochemical at the scale of the chondrules and matrix, likely confined to zones within 100–200 μm around anhydrous chondrules. Moreover, Hirakawa et al. [52] proved that organic matter–mineral interaction could also lead to in-situ aqueous alteration through water generation by decomposition of organic compounds with hydroxy groups after heating. In this case, it forms locally hydrated phyllosilicates on the surface of olivine in carbonaceous chondrites.

Most of the chondrites have an ultramafic composition, and their dominant aqueous alteration is the serpentinization of olivine and pyroxene. On Earth, this process is controlled at an early stage by the chemical potentials of water, silica, and oxygen, which determine the presence or absence of the associated phases, brucite and magnetite [53]. Since serpentinization in chondrites is nearly isochemical, it is considered to operate in closed systems [13,51,54]. Consequently, polyphased assemblages should be formed, i.e., serpentine must be associated with a Fe-rich mineral phase. The most open systems are found in the veins, which crosscut the chondrite body. In this case, the phyllosilicates are Fe- and Mg-rich; for example, chlorite or chlorite/saponite mixed layer minerals have been identified in vein deposits in the Orgueil meteorite [55].

Serpentine is classically thought to be the alteration product of olivine reacting with water [12]. Thus, serpentinization occurring at temperatures below the stability field of forsterite + H_2O is strictly retrogressive. Consequently, serpentine and olivine are considered to form alternatively and never simultaneously. However, the reverse reaction exists in thermal metamorphism environments where serpentine participates in dehydration reactions, forming olivine. Antigorite and olivine crystals have been observed to crystallize concomitantly in chrysotile veins [56]. Antigorite is the high-temperature polymorph of serpentine phases, and is stable up to extreme pressure–temperature conditions in the Earth's mantle [57]. Its composition varies between Mg and Fe end-members, but the Fe^{2+} for Mg substitution is favored by low temperatures in systems in which hydrogen and water fugacities are low and high, respectively [58,59].

On Earth, the isochemical alteration of olivine at high temperatures ($T > 300\text{ }^\circ\text{C}$) produces two secondary phases sharing the Fe and Mg components: antigorite and brucite, which are richer in Mg and Fe, respectively, than the parent olivine [60]. Brucite has not been detected in chondrites; however, the Fe-rich phase present is cronstedtite. This implies that silica activity is high enough to inhibit the formation of Mg and Fe hydroxide and to favor that of a phyllosilicate. For instance, some serpentine minerals in chondrites are intergrown with saponite [10,19], and saponite is known to crystallize in ultramafic rocks at a temperature higher than $400\text{ }^\circ\text{C}$ [53], provided the silica activity is higher than that required for cronstedtite formation.

The most commonly encountered species of the smectite family in carbonaceous chondrite (CC) are saponite and nontronite. They are also found in Martian Nakhilite meteorites [61]. These smectites are frequently observed in weathered or hydrothermally altered mafic-ultramafic rocks on Earth, where they are considered to be markers of low-temperature aqueous alteration processes ($<300\text{ }^\circ\text{C}$). However, saponite has been synthesized up to $800\text{ }^\circ\text{C}$ (1kbar) in association with talc and anthophyllite [62,63]. These high-temperature syntheses were carried out over short periods (20 days maximum) in potassium-depleted systems because potassium favors the formation of micas. Whitney [64] has shown that the temperatures at which saponite forms are low ($400\text{ }^\circ\text{C}$) if the reaction time is multiplied by 10 (200 days).

Kloprogge et al. [65] summarized data from different experimental syntheses of trioctahedral smectites through composition–temperature phase diagrams (1 kbar fixed pressure; $200\text{--}800\text{ }^\circ\text{C}$). They showed that nontronite might also form in high-temperature conditions, even though most available data are relative to low-temperature synthesis. Decarreau et al. [44] synthesized nontronite up to $200\text{ }^\circ\text{C}$ simultaneously with pyroxene. Accordingly, saponite and nontronite formation is kinetically controlled and may be concomitant with that of anhydrous silicates (pyroxene).

2.4. Alternative Interpretations of Chondrule Rim Petrographical Features

The aqueous alteration in chondrites is well-established, and its intensity has been used to classify the CM chondrites [66]. However, the source of water remains questionable: is it external or internal to the chemical system? Some petrographical features considered to result from alterations triggered by external water sources are questionable. These concerns are addressed in the following sections.

Several sources of water within meteorite parent bodies can explain the presence of phyllosilicates and other phases formed from aqueous fluids, such as carbonates, phosphates, and magnetite. One possibility is that molten ice accreted within the parent body, as suggested by Grimm and McSween [67]. Alternatively, water-bearing phyllosilicates may have formed directly in the solar nebula [17,68,69]. Once incorporated, the water begins to react with the surrounding material, silicates, metals, and sulfides, at relatively low temperatures. Various heat sources, such as the decay of ^{26}Al [70], short-lived local heating events caused by impacts, or solar radiation [71], can result in low aqueous alteration temperatures ranging from 0 to 150 °C for CI and CM chondrites [72,73]. Thus, the origin of the water is probably multi-origin in the composition of phyllosilicate, forming CI and CM chondrites.

While olivine is commonly found in meteorites, the ferrous iron-rich end-member, fayalite (Fe_2SiO_4), has been identified only as a minor secondary mineral in certain unequilibrated ordinary and carbonaceous chondrites [74]. Fayalite (Fe_2SiO_4) holds significant importance among secondary minerals since it serves as a proxy for the composition of the fluid in which it originated. This is attributed to its low fractionation factor, $\alpha_{\text{Fa-water}}$ [75], particularly within the temperature range typically associated with fayalite formation, which is estimated to be between 100 and 300 °C [74,76]. Within various unequilibrated ordinary chondrites, fayalite exhibits a close association with silica-rich chondrules/clasts, often forming veins, rims, layers, and lacy networks surrounding them (Figure 5a,b). Typically, fayalite coexists with magnetite (except at low W/R ratios), phyllosilicates, troilite, phosphates (such as whitlockite), chromite, Ca-Fe-rich pyroxene, and condensed organic compounds. In chondrites, two distinct origins of fayalite have been proposed: gas-melt interactions or aqueous alteration. According to Krot et al. [77], the high-temperature interactions between nebular gas and chondrites fail to explain the formation of fayalite-hedenbergite veinlets observed in CO and CM chondrites. They propose aqueous alteration as the likely origin of fayalite formation. The point discussed here is derived from an example in the Vigarano CV3 carbonaceous chondrite [78].

Fayalite-troilite-magnetite veinlets intrude into olivine-rich fine-grained rims (FGRs) (Figure 5a,b). Magnetite crystals are thought to have been largely replaced by fayalite due to their irregular form (Figure 5c,d). Consequently, the Vigarano chondrite is thought to feature two generations of veins, i.e., magnetite-troilite veins that have been later changed by fayalite-bearing veins. If this is true, the two vein types exhibiting identical morphologies should have genetic relationships in a decreasing temperature sequence of water/rock interactions. This two-step scenario is based on the interpretation of irregularly shaped magnetite crystals as fingerprints of an incomplete alteration state (retreating surfaces). However, the magnetite crystals are embedded inside the fayalite ones without any visible porosity at the observation scale (Figure 5d), giving the vein a compact texture similar to those in magmatic rocks. Such irregular shapes are commonly observed on Earth in magmatic rocks exhibiting skeletal crystals, which result from incomplete crystal growth (Figure 1). Skeletal crystals are typical of quenched magmatic bodies. Because there are no deformation features or crystal fracturing present, the veining is attributed to local fluid overpressure rather than mechanical stress (such as impact shock). In other words, the fayalite-troilite-magnetite veinlets have formed by opening pathways inside the rims. Another question emerges at this point: are these veinlets hydrothermal or magmatic in origin? Thermodynamical calculation shows that fayalite can form in anhydrous as well as hydrated systems. The origin of fayalite (Fa) in ordinary and CV3 carbonaceous chondrites is compatible with an aqueous alteration process below 350 °C only for a narrow

range of water/rock ratios [74]. In a hydrothermal context, the higher the Fa content, the higher the water/rock and H_2/H_2O ratios. Since most of the fayalite crystals are $Fa > 80$ in the veinlets, their temperature of crystallization varies from 150 to 200 °C for a given water/rock ratio [74]. The parent material (matrix) in the Vigarano chondrite is fine-grained (approximately 100 μm thick) and predominantly composed of olivine (Fa_{40-60}) or saponite, both of which are Mg-rich minerals [78]. This eliminates hydrothermal dissolution, which unavoidably would have produced Mg-rich solutions. Metamorphic reactions are not possible because Fe-rich serpentine is not present in the matrix, and the texture of veinlets is not compatible with a metamorphic origin.

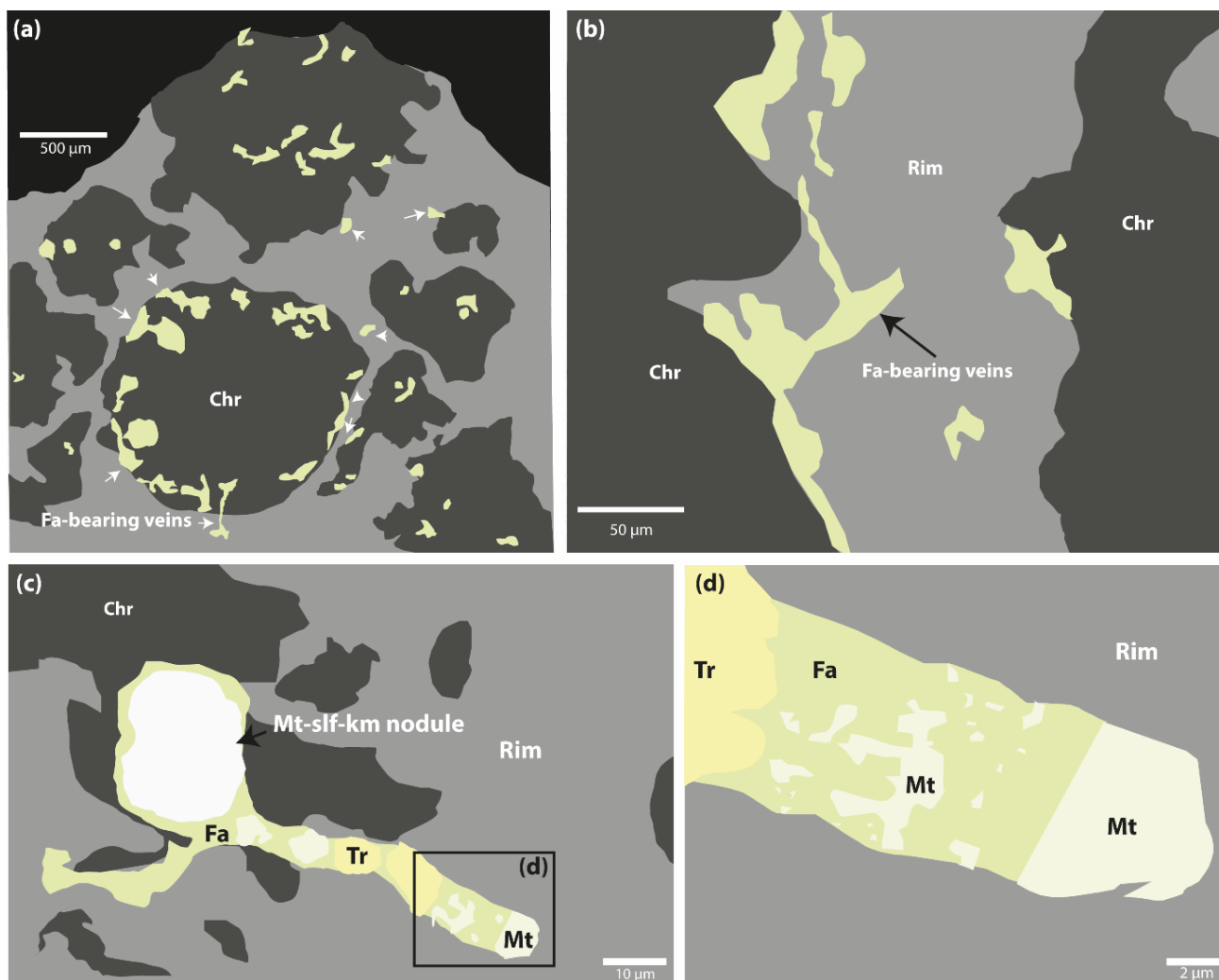


Figure 5. Schematic representation of backscattered electron (BSE) images of representative CV3 Vigarano chondrite. (a) Schematic reconstruction illustrating the occurrence of Fayalite (Fa) as veins and a lacy network surrounding the chondrules in the CV3 Vigarano chondrites (white arrows) (reconstruction of Figure 1 in [78]). (b) Fayalite bearing veins crosscut rims in the space between two chondrules. (c) A vein composed of fayalite (Fa), troilite (Tr), and magnetite (Mt) emerges from a magnetite–sulfide–kamacite (mt-slf-km) nodule. (d) A part of (c) between large troilite and magnetite grains, small fayalite grains coexist with irregularly shaped magnetites ((b–d) are modified from Figure 2 in [78]).

On Earth, the fayalite-magnetite assemblage is found in two distinct settings: hydrothermal veins crosscutting massive sulfide deposits [79] and within the carbonatite magmatic series [80]. The formation temperature conditions are 300 °C and > 500 °C, respec-

tively. The composition of the carbonatite magma progressively evolves into hypersaline fluids, creating a continuum between magmatic and hydrothermal fluids.

All of the fayalite-troilite-magnetite veinlets in the Vigarano chondrite extend from magnetite-sulfide or magnetite-sulfide-kamacite nodules. These nodules do not exhibit any dissolution features, indicating that they were the nucleating sites of the veinlets but not their parent material. Thus, the source of the fayalite-troilite-magnetite assemblage would have been necessarily related to the formation of the chondrules. The droplets of ultramafic-type melt reached a temperature near the liquidus, from 1350 to 1800 °C, depending on the duration of heating [13], and then cooled very quickly at 10 to 1000 K/hour [17]. The veinlets could represent the last crystallization step of a residual ferro-magnesian magmatic liquid at the end of the cooling stage.

Another example of aqueous alteration features can be observed in carbonaceous chondrites GUE 97,990 and Y 791,198 CM. This alteration is characterized by a mesostasis comprising quenched crystallites within chondrules. These chondrules mainly consist of phenocrysts of olivine and enstatite, with minor amounts of diopside [81]. The mesostasis is composed of dense arrays of parallel lath-shaped crystallites of diopside regularly alternating with serpentine (Figure 6a). The serpentine is thought to result from the aqueous alteration of pre-existing material. Since olivine and enstatite phenocrysts are not altered inside their bodies or at contact with mesostasis, the pre-existing material is assumed to be silicate glass. The phenocrysts remain unaltered because of their higher resistance to aqueous alteration compared to glassy mesostasis [66].

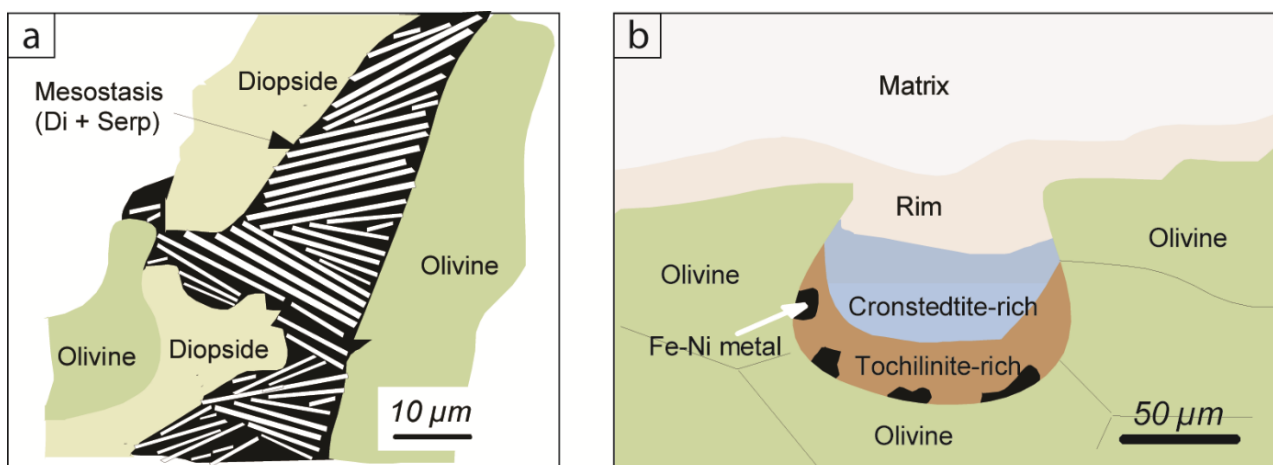


Figure 6. Schematic representations of petrographical features observed in the QUE97990 chondrite [81]. (a) Chondrule mesostasis is formed of dense arrays of parallel lath-shaped crystallites of diopside regularly alternating with serpentine (modified from Figure 1 in [81]). Such a petrographical feature could be a symplectite. (b) Embayment in chondrules exhibiting zoned mineral deposits (modified from Figure 2c in [81]). The embayment could be inherited from the initial shape of the chondrule. The zoned deposit could be formed by thermal metamorphism.

Similar alteration features are observed on Earth in oceanic basalts, where the interstitial glass is replaced by saponite while the outer surfaces of the phenocrysts remain intact [82]. This alteration process is non-isochemical and has been observed to involve the uptake of Mg and Fe, as well as the loss of Si and Al, with little or no leaching of alkalis. The chemical reactions are controlled by the high concentrations of Na and Mg in the solution, i.e., seawater (an infinite reservoir). It is evident that such control by the fluid composition is not feasible in the GUE 97,990 and Y 791,198 chondrites due to the limited availability of water. Consequently, the alteration of the chondrule mesostasis is controlled by the composition of the pre-existing material (a nearly closed system). Considering that chemical reactions in closed systems typically yield polyphase assemblages, the formation of a monophase assemblage is only feasible when the initial material closely resembles

its resulting secondary product, such as serpentine. Such a glass composition does not occur naturally on Earth, not even in komatiitic magmas [83]. For instance, in spinifex-textured komatiites, some olivine crystals undergo substantial replacement by serpentine and magnetite upon serpentinization [84]. This excludes aqueous alteration as the origin of serpentine. A possible explanation for the particular serpentine-diopside texture may be the co-precipitation of the two components forming a symplectite (Figure 6a). In this case, the symplectite represents a metastable eutectic assemblage, as suggested by Rietmeijer et al. [85].

The fine-grained rims (FGRs) identified in CI and CM chondrites comprise an un-equilibrated fine grained assemblage with variable amounts of Mg-Fe amorphous silicates and phyllosilicates, along with anhydrous silicates, sulfides, metals, and organic compounds [86,87]. FGRs share similar phase compositions with the matrix; however, they display distinct textures, including variations in grain size, compaction, porosity, and presolar grain abundances [88]. This disparity suggests that they may have originated from similar materials but experienced differing conditions during their formation [86,89]. FGRs are thought to be formed by dust accretion onto the surface of chondrules prior to their incorporation into the matrix [87]. On the other hand, other researchers have proposed mechanisms such as alteration at the chondrule/matrix interface within the parent body or the compaction of dust surrounding chondrules within regoliths [90–92]. Hydrated and anhydrous regions are contiguous, suggesting that rims have accreted material from multiple reservoirs [17,93,94]. Differences in chemical composition between the matrix and rim are often attributed to the transfer of elements from the chondrule to its associated rim [95]. However, these chemical transfers alone may not be sufficient to result in a substantial difference in the mineralogical composition of FGRs compared to their host matrix. The preservation of the mineralogical composition suggests that the changes in physical–chemical–time conditions during the transfer of elements were not high enough to induce the formation of new mineral phases. FGRs are often characterized by the recrystallization of pre-existing phases, which may change in composition (Fe oxidation in saponite) and crystal size (ripening). Unfortunately, while changes in composition can be readily measured, quantifying the effects of ripening is far more challenging. Qualitative observations of most CM chondrites show grain coarsening (with some exceptions). Even if grain coarsening needs less energy than mineral reactions, it indicates that alteration occurred at rather high temperatures, in high water/rock ratios, or for long periods of time [86]. Are the recrystallizations observed in the FGRs consistently attributed to aqueous alteration? In other words, do retreating surfaces exist? For example, this question leads to research on the origin of the pyroxene and olivine crystal embayments of the CV3 Vigarano chondrite (Figure 6b) [96]. Embayments (topographic depressions in the chondrules) are considered to be dissolved zones filled by alteration products, i.e., phyllosilicate-rich materials. The aqueous alteration origin is coherent with the presence of Fe hydroxide veinlets forming in Fe-Ni metals, magnetite, and Fe sulfide grains. However, the embayments in some chondrules of the GUE 97,990 and Y 791,198 chondrites are filled by tochilinite- and cronstedtite-rich materials, which also contain fine grains (5 μm) of forsterite-rich olivine, pyroxene, Ca-carbonate, troilite, pentlandite, and Fe-Ni metal [81]. In many of the embayments, the rims exhibit a distinct enrichment in iron compared to other parts of the rims [81]. Fe-Ni metallic grains are concentrated at the interface between the chondrule olivine crystals and their associated rim (Figure 5b). These embayments were interpreted as formations resulting from the replacement of opaque nodules within their host chondrules through aqueous alteration. However, some problems remain. Indeed, since the Fe-Ni metal grains are highly unstable in the presence of water [97], their presence is not consistent with an aqueous alteration origin. During the formation of the chondrules, the metal grains migrate toward the melt–FGRs interface [98]. Their concentration along the embayment–FGRs interface in the GUE 97,990 and Y 791,198 chondrites could indicate that the embayment is not a dissolution feature but is inherited from the initial shape of the chondrule. If this is the case, the tochilinite-cronstedtite deposit sequence would result

from thermal metamorphism rather than aqueous alteration. Zoning is frequently observed in thermal metamorphic rocks, where chemical diffusion is activated. Mineral reactions are controlled by the gradients of chemical potentials between the heat source and the host material. In the present case, the observed zoning (tochilinite-rich to cronstedtite-rich, Figure 6b) could be due to the decrease of sulfur chemical potential with distance to interface, supported by the decrease of S from tochilinite-rich, which is in contact with the chondrule, to cronstedtite-rich, which is at the interface between the embayment and the FGRs (Table 1). Moreover, the presence of pyroxene, carbonate, and troilite small grains in the FGR suggests thermal metamorphism rather than an aqueous alteration environment in which they are unstable.

Table 1. EDS analyses of materials in the chondrule embayments and rims in the QUE 97,990 chondrite.

	Embayments		Rims
	Tochilinite-Rich	Cronstedtite-Rich	Mg-Fe Serpentine-Rich
Number of Analysis	20	21	35
SiO ₂	3.47 (±0.99)	20.3 (±3.3)	24.3 (±1.9)
TiO ₂	0.14 (±0.05)	0.11 (±0.09)	0.11 (±0.09)
Al ₂ O ₃	0.55 (±0.14)	3.98 (±0.87)	2.87 (±0.48)
Cr ₂ O ₃	1.78 (±1.09)	0.61 (±0.92)	0.44 (±0.17)
FeO	46.1 (±2.9)	40.6 (±11.4)	25.2 (±1.7)
NiO	11.1 (±1.7)	2.09 (±1.62)	2.59 (±0.54)
MnO	1.15 (±0.33)	1.00 (±0.39)	0.18 (±0.21)
MgO	3.83 (±0.47)	8.91 (±2.93)	14.4 (±1.8)
CaO	0.73 (±0.17)	0.50 (±0.50)	1.03 (±0.28)
Na ₂ O	0.13 (±0.07)	0.36 (±0.23)	0.16 (±0.12)
S	15.6 (±1.1)	2.92 (±1.48)	4.08 (±0.70)
Total	84.6	84.4	75.4

To conclude, the FGRs are distinguished from their host matrices by a less porous texture. Densification is classically considered to be the effect of the accretion of dust onto chondrules. However, in some cases, it could be due to thermal metamorphism. During cooling, a chondrule loses heat, which triggers the formation or recrystallization of some minerals in the host matrix. Even if most of the mineral species present in the matrix are conserved, some of them change in crystal size and composition. The process is not perfectly isochemical. Volatile siderophile and chalcophile elements are transferred from the chondrule [51,99].

3. Conclusions

The presence of phyllosilicates and, specifically, clay minerals in terrestrial rocks, as well as in chondrites, does not systematically imply aqueous alteration. Moreover, aqueous alteration does not necessarily imply exterior water inputs to the reacting system. Considering these two statements, the challenge lies in determining a plausible mechanism for carbonaceous chondrule formation. Phyllosilicates constitute about 50% of the cosmic dust [100,101]. They are considered to have been formed in the outer icy region of the nebula, during a previous alteration process, or as a result of asteroidal impacts [102]. They are deuterium-rich, as demonstrated by studies on Semarkona and Renazzo meteorites [103]. Phyllosilicates are the principal source of water in the hotter regions of the protoplanetary disk, with a water fraction possibly exceeding 10% [68]. Recent studies show that other crystalline or amorphous silicate components in IDPs can also serve as potential carriers of water through physi-sorbed molecules on their surfaces [104]. This suggests that the presence of water is highly probable in the dust agglomerates in which the chondrules and their associated FGRs form. The matrix exhibits a highly variable composition because of the amount of volatile components, which depends on the intensity of evaporation during

the chondrule-forming process [105]. Depending on the degree of melting and the intensity of back reactions between the chondrule and evaporating gas [106], the mineral reactions in the chondrule-forming process may occur either in water-poor or water-rich systems. This determines the presence or absence of hydrated minerals in the chondrule and its associated FGRs.

Summarizing the main steps in the formation of chondrules can be proposed in order to address the following questions (Figure 7): (1) Is aqueous alteration of chondrites analogous to terrestrial alteration processes? (2) Could non-aqueous alteration processes lead to the formation of Fe- and Mg-rich phyllosilicate in chondrites? (3) What are the specific physical-chemical conditions conducive to the formation of Fe and Mg clays?

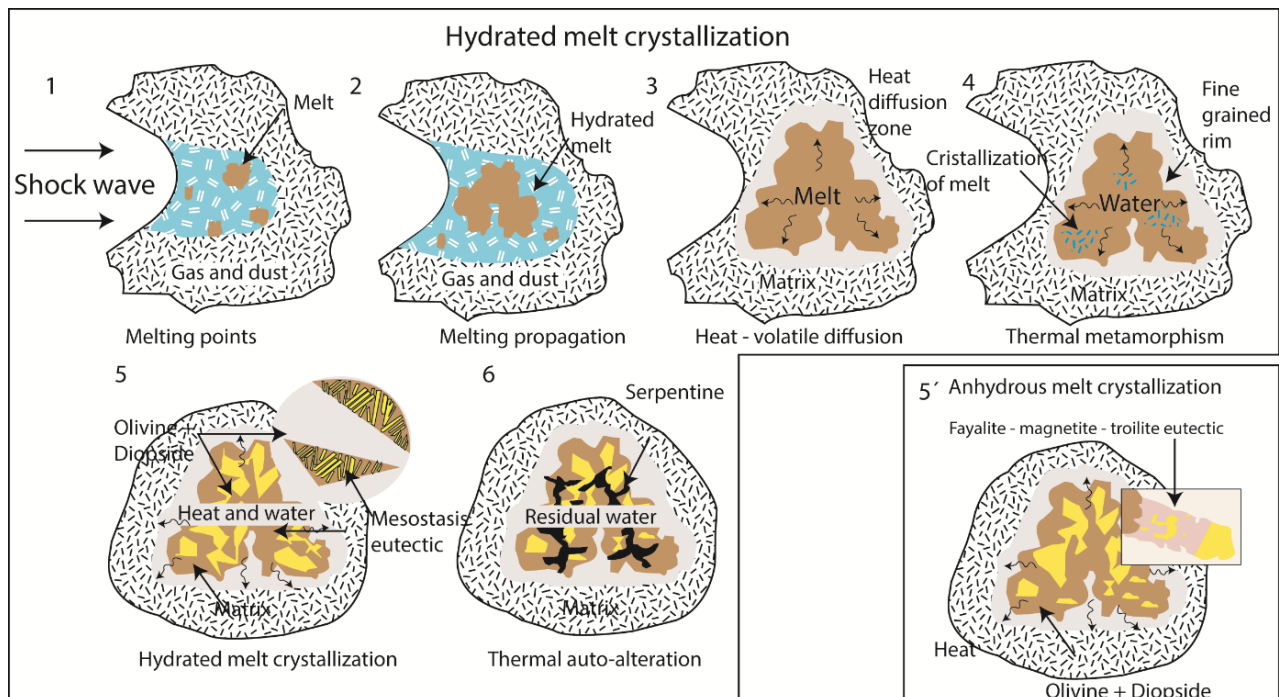


Figure 7. A schematic representation of a possible scenario for the formation of chondrules, describing the melting, crystallization, and alteration processes of hydrated materials.

3.1. Nucleation and Propagation of Melting

Chondrules exhibit spherical or multilobate shapes. According to Rubin and Wasson [107], the collapse into spheres is very rapid (10^{-3} s). Since this timeframe does not align with the crystallization time required for olivine phenocrysts to reach their size, the authors conclude that the presence of multilobate chondrules in CO chondrites is attributed to the partial re-melting of chondrule fragments. Such a multi-melting process inevitably results in an increasing loss of volatile components. Is this the only way to form multilobate chondrules? Melting experiments on fine-grained materials conducted by Ivanov and Zhigilei [108,109] show that melt nucleation occurs at several points and forms a melting front, resulting in a highly irregular surface over time. In this case, the melting process is more conservative with respect to volatile components compared to the multi-melting approach (closed system).

Macroscopically, the propagation of the melting fronts from the initial melting points within a fine-grained material leads to the coalescence of the melted zones. The resulting irregularly shaped proto-chondrule may exhibit deep embayments that entrap remnants of the unmelted matrix [110]. Consequently, it is plausible that the IDP agglomerates may initiate melting at several points under the influence of shock waves. The melting temperature ranges from 1400 to 1900 K, but the presence of water in the system may lower it.

3.2. Diffusion of Heat and Volatile Components from the Chondrule to the Matrix

During melting, the Fe-Ni metal grains migrate to the surface of the proto-chondrule [98]. Subsequently, heat and chemical components diffuse into the surrounding matrix, which is enriched in siderophile and chalcophile volatile components [51] and undergoes transformation through mineral reactions. The sulfur chemical potential gradient results in the formation of “thermally metamorphosed” rim zoning at the chondrule interface consisting of (1) tochilinite and (2) cronstedtite. The presence of fayalite-magnetite-troilite veinlets observed in the Vigarano carbonaceous chondrite suggests that the rim they intersect predates their formation. Therefore, rims are intimately associated with the early stages of proto-chondrule development.

The rim interfaces exhibit either sharp or progressive transitions between the chondrule and matrix, respectively. The “metamorphic” mineral reactions within the hosting matrix are thermally activated by heat diffusion from the chondrule, resulting in mineral zoning and increased density. This process is continuous until the latent heat of crystallization is dissipated. As the newly formed minerals in the melt (such as olivine and diopside) are anhydrous, volatile, and incompatible components, they gradually accumulate in the residual fluids. The “metamorphosed” rim, being less porous than the matrix, forms an impermeable coating that prevents rapid volatile loss. Due to the brutal quenching of the melt, a significant portion of the water expelled during crystallization remains within the system.

3.3. Final Crystallization Stage and Hydrothermal Auto-Alteration

According to Ciesla et al. [17], the cooling rates range from 10 to 1000 K/hour as the chondrule approaches the solidus (1400 K). The higher the cooling rate, the more dendritic the textures of olivine and diopside become, and the greater the amount of mesostasis. Intermediate cooling rates allow the crystallizing melt to reach the eutectic or metastable eutectic temperature [85]. Symplectites are typical eutectic micro-textures, and the nature of their mineral components depends on the quantity of water dissolved in the residual magmatic liquid. If water is lacking, the eutectic composition is entirely composed of anhydrous silicates, oxides, and sulfides. This is the case for the Vigarano carbonaceous chondrite, in which the final magmatic stage produces fayalite-magnetite-troilite veinlets that invade the metamorphosed rim [78]. If the water activity is high, it does not allow the formation of olivine-fayalite but favors that of serpentine. In this case, the eutectic symplectite is formed of serpentine and diopside. This is the case of the QUE97990 carbonaceous chondrite [81].

In some cases, water is not consumed in the eutectic minerals due to rapid quenching but rather becomes concentrated in the residual fluid, impregnating microcracks and intergranular joints in the chondrule. Equilibrium is maintained between the resident fluids and the hosting minerals until the temperature drops to a critical value (350 K). At this point, as olivine loses its stability in the presence of water, it undergoes a reaction, resulting in the formation of serpentine. Serpentinization progresses from fractures towards the interior of the crystal body as long as water remains available in the system. This phenomenon is referred to as “auto-alteration”, and it occurs without requiring any external water input, making it a closed system process.

Author Contributions: A.E.A. and A.M. designed the research. A.E.A., A.M., F.W., M.G., I.C., C.F., F.A., E.H.B., O.B., J.N.I., A.E.K., A.A.E. and H.C.A., collected, compiled, and analyzed the data. A.E.A., I.C. and A.M., wrote the manuscript with the contribution of the co-authors. All authors have read and agreed to the published version of the manuscript.

Funding: This work was supported by La Région Nouvelle Aquitaine (Project “Darwin”, grant E137CR21), l’Agence Nationale de la Recherche Scientifique (BIOGEN, grant ANR-22-CE49-0010-02), and the French government program (Investissements d’Avenir EUR INTREE, ANR-18-EURE-0010).

Data Availability Statement: All data generated or analyzed during this study are included in this published article.

Acknowledgments: The Moroccan Hassan II Academy of Sciences and Technology and the Moroccan Ministry of Energy and Mines are thanked for their collaboration and support. We thank Javier Cuadros and two anonymous reviewers for their valuable feedback during the review process, and Sutita Changsing and Charisma Lu for editorial handling. We thank C. Lebailly, L. Tromas, and C. Laforest for assistance.

Conflicts of Interest: The authors declare no conflict of interest.

References

1. Grady, M.; Pratesi, G.; Moggi Cecchi, V. *Atlas of Meteorites*; Cambridge University Press: Cambridge, UK, 2014.
2. Krot, A.N.; Keil, K.; Scott, E.R.D.; Goodrich, C.A.; Weisberg, M.K. Classification of meteorites and their genetic relationships. In *Treatise on Geochemistry*, 2nd ed.; Holland, D.H., Turekian, K.K., Eds.; Elsevier: Amsterdam, The Netherlands, 2014; Volume 1, pp. 1–63, ISBN 9780080959757.
3. Wiik, H. The chemical composition of some stony meteorites. *Geochim. Cosmochim. Acta* **1956**, *9*, 279–289. [[CrossRef](#)]
4. Braukmüller, N.; Wombacher, F.; Hezel, D.C.; Escoube, R.; Münker, C. The chemical composition of carbonaceous chondrites: Implications for volatile element depletion, complementarity and alteration. *Geochim. Cosmochim. Acta* **2018**, *239*, 17–48. [[CrossRef](#)]
5. Weisberg, M.K.; McCoy, T.J.; Krot, A.N. Systematics and evaluation of meteorite classification. In *Meteorites and the early Solar System II*; Lauretta, D.S., McSween, H.Y., Jr., Eds.; University of Arizona Press: Tucson, AZ, USA, 2006.
6. Anders, E.; Ebihara, M. Solar-system abundances of the elements. *Geochim. Cosmochim. Acta* **1982**, *46*, 2363–2380. [[CrossRef](#)]
7. Anders, E.; Grevesse, N. Abundances of the elements: Meteoritic and solar. *Geochim. Cosmochim. Acta* **1989**, *53*, 197–214. [[CrossRef](#)]
8. Barber, D.J. Phyllosilicates and other layer-structured materials in stony meteorites. *Clay Miner.* **1985**, *20*, 415–454. [[CrossRef](#)]
9. Brearley, A.J. The Action of Water. *Meteor. Early Sol. Syst. II* **2006**, *943*, 587–624.
10. Buseck, P.R.; Hua, X. Matrices of Carbonaceous Chondrite Meteorites. *Annu. Rev. Earth Planet. Sci.* **1993**, *21*, 255–305. [[CrossRef](#)]
11. Nuth III, J.A.; Brearley, A.J.; Scott, E.R. Microcrystals and Amorphous Material in Comets and Primitive Meteorites: Keys to Understanding Processes in the Early Solar System. *Proc. Chondrites Protoplanetary Disk* **2005**, *341*, 675.
12. Beck, P.; Quirico, E.; Montes-Hernandez, G.; Bonal, L.; Bollard, J.; Orthous-Daunay, F.-R.; Howard, K.; Schmitt, B.; Brissaud, O.; Deschamps, F.; et al. Hydrous mineralogy of CM and CI chondrites from infrared spectroscopy and their relationship with low albedo asteroids. *Geochim. Cosmochim. Acta* **2010**, *74*, 4881–4892. [[CrossRef](#)]
13. Scott, E.R. Chondrites and the Protoplanetary Disk. *Annu. Rev. Earth Planet. Sci.* **2007**, *35*, 577–620. [[CrossRef](#)]
14. Kleine, T.; Rudge, J.F. Chronometry of Meteorites and the Formation of the Earth and Moon. *Elements* **2011**, *7*, 41–46. [[CrossRef](#)]
15. Trigo-Rodríguez, J.M.; Rimola, A.; Tanbakouei, S.; Soto, V.C.; Lee, M. Accretion of Water in Carbonaceous Chondrites: Current Evidence and Implications for the Delivery of Water to Early Earth. *Space Sci. Rev.* **2019**, *215*, 18. [[CrossRef](#)]
16. Ohnishi, I.; Tomeoka, K. Dark inclusions in the Mokoia CV3 chondrite: Evidence for aqueous alteration and subsequent thermal and shock metamorphism. *Meteorit. Planet. Sci.* **2002**, *37*, 1843–1856. [[CrossRef](#)]
17. Ciesla, F.J.; Lauretta, D.S.; Cohen, B.A.; Hood, L.L. A Nebular Origin for Chondritic Fine-Grained Phyllosilicates. *Science* **2003**, *299*, 549–552. [[CrossRef](#)] [[PubMed](#)]
18. Cohen, B. Modeling of Liquid Water on CM Meteorite Parent Bodies and Implications for Amino Acid Racemization. *Icarus* **2000**, *145*, 369–381. [[CrossRef](#)]
19. Scott, E.R.D.; Krot, A.N. Chondrites and Their Components. *Treatise Geochem.* **2003**, *1*, 711.
20. Pignatelli, I.; Mugnaioli, E.; Marrocchi, Y. Cronstedtite polytypes in the Paris meteorite. *Eur. J. Miner.* **2018**, *30*, 349–354. [[CrossRef](#)]
21. Meunier, A.; Mas, A.; Beaufort, D.; Patrier, P.; Dudoignon, P. Clay Minerals in Basalt-Hawaiite Rocks From Mururoa Atoll (French Polynesia). II. Petrography and Geochemistry. *Clays Clay Miner.* **2008**, *56*, 730–750. [[CrossRef](#)]
22. Mas, A.; Meunier, A.; Beaufort, D.; Patrier, P.; Dudoignon, P. Clay Minerals in Basalt-Hawaiite Rocks From Mururoa Atoll (French Polynesia). I. Mineralogy. *Clays Clay Miner.* **2008**, *56*, 711–729. [[CrossRef](#)]
23. Turpault, M.; Meunier, A.; Guilhaumou, N.; Touchard, G. Analysis of hot fluid infiltration in fractured granite by fluid inclusion study. *Appl. Geochem.* **1992**, *7*, 269–276. [[CrossRef](#)]
24. Meunier, A.; Sardini, P.; Robinet, J.C.; Prêt, D. The petrography of weathering processes: Facts and outlooks. *Clay Miner.* **2007**, *42*, 415–435. [[CrossRef](#)]
25. Banfield, J.F.; Barker, W.W. Direct observation of reactant-product interfaces formed in natural weathering of exsolved, defective amphibole to smectite: Evidence for episodic, isovolumetric reactions involving structural inheritance. *Geochim. Cosmochim. Acta* **1994**, *58*, 1419–1429. [[CrossRef](#)]
26. Proust, D.; Caillaud, J.; Fontaine, C. Clay Minerals in Early Amphibole Weathering: Tri- to Dioctahedral Sequence as a Function of Crystallization Sites in the Amphibole. *Clays Clay Miner.* **2006**, *54*, 351–362. [[CrossRef](#)]
27. Velbel, M.A. Weathering of Hornblende to Ferruginous Products by a Dissolution-Reprecipitation Mechanism: Petrography and Stoichiometry. *Clays Clay Miner.* **1989**, *37*, 515–524. [[CrossRef](#)]
28. Eggleton, R.A.; Boland, J.N. Weathering of Enstatite to Talc through a Sequence of Transitional Phases. *Clays Clay Miner.* **1982**, *30*, 11–20. [[CrossRef](#)]
29. Velbel, M.A. Dissolution of olivine during natural weathering. *Geochim. Cosmochim. Acta* **2009**, *73*, 6098–6113. [[CrossRef](#)]

30. Putnis, A. Mineral replacement reactions: From macroscopic observations to microscopic mechanisms. *Mineral. Mag.* **2002**, *66*, 689–708. [[CrossRef](#)]
31. Velbel, M.A.; Barker, W.W. Pyroxene weathering to smectite: Conventional and cryo-field emission scanning electron microscopy, Koua Bocca ultramafic complex, Ivory Coast. *Clays Clay Miner.* **2008**, *56*, 112–127. [[CrossRef](#)]
32. Drief, A.; Schiffman, P. Very low-temperature alteration of sideromelane in hyaloclastites and hyalotuffs from Kilauea and Mauna Kea volcanoes: Implications for the mechanism of palagonite formation. *Clays Clay Miner.* **2004**, *52*, 622–634. [[CrossRef](#)]
33. Goff, F. Vesicle cylinders in vapor-differentiated basalt flows. *J. Volcanol. Geotherm. Res.* **1996**, *71*, 167–185. [[CrossRef](#)]
34. Gualtieri, A.F.; Gemmi, M.; Dapiaggi, M. Phase transformations and reaction kinetics during the temperature-induced oxidation of natural olivine. *Am. Miner.* **2003**, *88*, 1560–1574. [[CrossRef](#)]
35. Caroff, M.; Maury, R.C.; Cotten, J.; Clément, J.-P. Segregation structures in vapor-differentiated basaltic flows. *Bull. Volcanol.* **2000**, *62*, 171–187. [[CrossRef](#)]
36. Clément, J.-P.; Caroff, M.; Dudoignon, P.; Launeau, P.; Bohn, M.; Cotten, J.; Blais, S.; Guille, G. A possible link between gabbros bearing High Temperature Iddingsite alteration and huge pegmatoid intrusions: The Society Islands, French Polynesia. *Lithos* **2007**, *96*, 524–542. [[CrossRef](#)]
37. Meunier, A. Clays in Sedimentary Environments. In *Clays*; Springer: Berlin/Heidelberg, Germany, 2005; pp. 295–327, ISBN 978-3-540-27141-3.
38. Alt, J.C. Very Low-Grade Hydrothermal Metamorphism of Basic Igneous Rocks. In *Low-Grade Metamorphism*; Blackwell Pub: Vestavia Hills, AL, USA, 1999; pp. 169–201.
39. Neuhoff, P.S. Porosity evolution and mineral paragenesis during low-grade metamorphism of basaltic lavas at Teigarhorn, eastern Iceland. *Am. J. Sci.* **1999**, *299*, 467–501. [[CrossRef](#)]
40. Goltz, A.E.; Krawczynski, M.J.; Gavrilenko, M.; Gorbach, N.V.; Ruprecht, P. Evidence for superhydrous primitive arc magmas from mafic enclaves at Shiveluch volcano, Kamchatka. *Contrib. Miner. Pet.* **2020**, *175*, 1–26. [[CrossRef](#)]
41. Grigor'ev, D.P. *Ontogeny of Minerals: Israel Program for Scientific Translations*; Davey: Jerusalem, Israel, 1965.
42. Meunier, A.; Petit, S.; Ehlmann, B.L.; Dudoignon, P.; Westall, F.; Mas, A.; El Albani, A.; Ferrage, E. Magmatic precipitation as a possible origin of Noachian clays on Mars. *Nat. Geosci.* **2012**, *5*, 739–743. [[CrossRef](#)]
43. Nakazawa, H.; Yamada, H.; Fujita, T. Crystal synthesis of smectite applying very high pressure and temperature. *Appl. Clay Sci.* **1992**, *6*, 395–401. [[CrossRef](#)]
44. Decarreau, A.; Petit, S.; Vieillard, P.; Dabert, N. Hydrothermal synthesis of aegirine at 200°C. *Eur. J. Miner.* **2004**, *16*, 85–90. [[CrossRef](#)]
45. De Leuw, S.; Rubin, A.E.; Wasson, J.T. Carbonates in CM chondrites: Complex formational histories and comparison to carbonates in CI chondrites. *Meteorit. Planet. Sci.* **2010**, *45*, 513–530. [[CrossRef](#)]
46. Tomeoka, K.; Buseck, P.R. Indicators of aqueous alteration in CM carbonaceous chondrites: Microtextures of a layered mineral containing Fe, S, O and Ni. *Geochim. Cosmochim. Acta* **1985**, *49*, 2149–2163. [[CrossRef](#)]
47. Tomeoka, K.; McSween, H.Y., Jr.; Buseck, P.R. Mineralogical Alteration of CM Carbonaceous Chondrites: A View. In *Proceedings of the NIPR Symposium on Antarctic Meteorites*; National Institute of Polar Research: Tachikawa, Japan, 1989; Volume 2, pp. 221–234.
48. Alexander, C.M.O.; Howard, K.T.; Bowden, R.; Fogel, M.L. The classification of CM and CR chondrites using bulk H, C and N abundances and isotopic compositions. *Geochim. Cosmochim. Acta* **2013**, *123*, 244–260. [[CrossRef](#)]
49. Young, E.D.; Zhang, K.K.; Schubert, G. Conditions for pore water convection within carbonaceous chondrite parent bodies – implications for planetesimal size and heat production. *Earth Planet. Sci. Lett.* **2003**, *213*, 249–259. [[CrossRef](#)]
50. Krot, A.N.; Hutcheon, I.D.; Brearley, A.J.; Pravdivtseva, O.V.; Petaev, M.I.; Hohenberg, C.M. *Timescales and Settings for Alteration of Chondritic Meteorites*; Lawrence Livermore National Lab. (LLNL): Livermore, CA, USA, 2005.
51. Bland, P.A.; Alard, O.; Benedix, G.K.; Kearsley, A.T.; Menzies, O.N.; Watt, L.E.; Rogers, N.W. Volatile fractionation in the early solar system and chondrule/matrix complementarity. *Proc. Natl. Acad. Sci. USA* **2005**, *102*, 13755–13760. [[CrossRef](#)] [[PubMed](#)]
52. Hirakawa, N.; Kebukawa, Y.; Furukawa, Y.; Kondo, M.; Nakano, H.; Kobayashi, K. Aqueous alteration without initial water: Possibility of organic-induced hydration of anhydrous silicates in meteorite parent bodies. *Earth Planets Space* **2021**, *73*, 1–11. [[CrossRef](#)]
53. Frost, C.D.; von Blanckenburg, F.; Schoenberg, R.; Frost, B.R.; Swapp, S.M. Preservation of Fe isotope heterogeneities during diagenesis and metamorphism of banded iron formation. *Contrib. Miner. Pet.* **2006**, *153*, 211–235. [[CrossRef](#)]
54. Velbel, M.A.; Tonui, E.K.; Zolensky, M.E. Replacement of olivine by serpentine in the Queen Alexandra Range 93005 carbonaceous chondrite (CM2): Reactant–product compositional relations, and isovolumetric constraints on reaction stoichiometry and elemental mobility during aqueous alteration. *Geochim. Cosmochim. Acta* **2015**, *148*, 402–425. [[CrossRef](#)]
55. Tomeoka, K. Metamorphic Processes in New CI Carbonaceous Chondrites from Antarctica: Mineralogy and Petrology. *Primit. Sol. Nebul. Orig. Planets* **1993**, 447–464.
56. Dungan, M.A. Metastability in Serpentine-Olivine Equilibria. *Am. Mineral.* **1977**, *62*, 1018–1029.
57. Grove, T.L.; Till, C.B.; Lev, E.; Chatterjee, N.; Médard, E. Kinematic variables and water transport control the formation and location of arc volcanoes. *Nature* **2009**, *459*, 694–697. [[CrossRef](#)]
58. Evans, B.W. Control of the Products of Serpentinization by the Fe²⁺+Mg-1 Exchange Potential of Olivine and Orthopyroxene. *J. Pet.* **2008**, *49*, 1873–1887. [[CrossRef](#)]

59. Evans, B.W.; Kuehner, S.M.; Chopelas, A. Magnetite-free, yellow lizardite serpentinization of olivine websterite, Canyon Mountain complex, N.E. Oregon. *Am. Miner.* **2009**, *94*, 1731–1734. [[CrossRef](#)]
60. Beard, J.S.; Frost, B.R.; Fryer, P.; McCaig, A.; Searle, R.; Ildefonse, B.; Zinin, P.; Sharma, S.K. Onset and Progression of Serpentinization and Magnetite Formation in Olivine-rich Troctolite from IODP Hole U1309D. *J. Pet.* **2009**, *50*, 387–403. [[CrossRef](#)]
61. Hicks, L.; Bridges, J.; Gurman, S. Ferric saponite and serpentine in the nakhlite martian meteorites. *Geochim. Cosmochim. Acta* **2014**, *136*, 194–210. [[CrossRef](#)]
62. Koizumi, M.; Roy, R. Synthetic Montmorillonoids with Variable Exchange Capacity*. *Am. Mineral.* **1959**, *44*, 788–805.
63. Iiyama, J.T.; Roy, R. Controlled Synthesis of Heteropolytypic (Mixed-Layer) Clay Minerals. *Clays Clay Miner. (Natl. Conf. Clays Clay Miner.* **1961**, *10*, 4–22. [[CrossRef](#)]
64. Whitney, G. Hydrothermal Reactivity of Saponite. *Clays Clay Miner.* **1983**, *31*, 1–8. [[CrossRef](#)]
65. Klopogge, J.T.; Komarneni, S.; Amonette, J.E. Synthesis of Smectite Clay Minerals: A Critical Review. *Clays Clay Miner.* **1999**, *47*, 529–554. [[CrossRef](#)]
66. Rubin, A.; Trigo-Rodríguez, J.; Huber, H.; Wasson, J. Progressive alteration of CM carbonaceous chondrites. *Geochim. Cosmochim. Acta* **2007**, *71*, 2361–2382. [[CrossRef](#)]
67. Grimm, R.E.; McSween Jr, H.Y. Water and the Thermal Evolution of Carbonaceous Chondrite Parent Bodies. *Icarus* **1989**, *82*, 244–280. [[CrossRef](#)]
68. Ciesla, F.; Lauretta, D. Radial migration and dehydration of phyllosilicates in the solar nebula. *Earth Planet. Sci. Lett.* **2005**, *231*, 1–8. [[CrossRef](#)]
69. Schneeberger, A.; Mousis, O.; Deleuil, M.; Lunine, J.I. Formation of the Trappist-1 system in a dry protoplanetary disk. *Astron. Astrophys.* **2024**, *682*, L10. [[CrossRef](#)]
70. McSween Jr, H.Y. Aqueous Alteration in Carbonaceous Chondrites: Mass Balance Constraints on Matrix Mineralogy. *Geochim. Cosmochim. Acta* **1987**, *51*, 2469–2477. [[CrossRef](#)]
71. Nakato, A.; Nakamura, T.; Kitajima, F.; Noguchi, T. Evaluation of dehydration mechanism during heating of hydrous asteroids based on mineralogical and chemical analysis of naturally and experimentally heated CM chondrites. *Earth Planets Space* **2008**, *60*, 855–864. [[CrossRef](#)]
72. Endress, M.; Zinner, E.; Bischoff, A. Early aqueous activity on primitive meteorite parent bodies. *Nature* **1996**, *379*, 701–703. [[CrossRef](#)] [[PubMed](#)]
73. Verdier-Paoletti, M.J.; Marrocchi, Y.; Avice, G.; Roskosz, M.; Gurenko, A.; Gounelle, M. Oxygen isotope constraints on the alteration temperatures of CM chondrites. *Earth Planet. Sci. Lett.* **2017**, *458*, 273–281. [[CrossRef](#)]
74. Zolotov, M.Y.; Mironenko, M.V.; Shock, E.L. Thermodynamic constraints on fayalite formation on parent bodies of chondrites. *Meteorit. Planet. Sci.* **2006**, *41*, 1775–1796. [[CrossRef](#)]
75. Zheng, Y.-F. “Calculation of Oxygen Isotope Fractionation in Anhydrous Silicate Minerals.” *Geochimica et Cosmochimica Acta. Geochim. Cosmochim. Acta* **1993**, *57*, 3199. [[CrossRef](#)]
76. Doyle, P.M.; Jogo, K.; Nagashima, K.; Krot, A.N.; Wakita, S.; Ciesla, F.J.; Hutcheon, I.D. Early aqueous activity on the ordinary and carbonaceous chondrite parent bodies recorded by fayalite. *Nat. Commun.* **2015**, *6*, 7444. [[CrossRef](#)] [[PubMed](#)]
77. Krot, A.N.; Brearley, A.J.; Petaev, M.I.; Kallemeyn, G.W.; Sears, D.W.; Benoit, P.H.; Hutcheon, I.D.; Zolensky, M.E.; Keil, K. Evidence for Low-Temperature Growth of Fayalite and Hedenbergite in MacAlpine Hills 88107, an Ungrouped Carbonaceous Chondrite Related to the CM-CO Clan. *Meteorit. Planet. Sci.* **2000**, *35*, 1365–1386. [[CrossRef](#)]
78. Jogo, K.; Nakamura, T.; Noguchi, T.; Zolotov, M.Y. Fayalite in the Vigarano CV3 carbonaceous chondrite: Occurrences, formation age and conditions. *Earth Planet. Sci. Lett.* **2009**, *287*, 320–328. [[CrossRef](#)]
79. Rasmussen, M.G.; Evans, B.W.; Kuehner, S.M. Low-Temperature Fayalite, Greenalite, and Minnesotaite from the Overlook Gold Deposit, Washington; Phase Relations in the System FeO-SiO₂-H₂O. *Can. Mineral.* **1998**, *36*, 147–162.
80. Goff, B.H.; Weinberg, R.; Groves, D.I.; Vielreicher, N.M.; Fourie, P.J. The Giant Vergenoeg Fluorite Deposit in a Magnetite-Fluorite-Fayalite REE Pipe: A Hydrothermally-Altered Carbonatite-Related Pegmatoid? *Mineral. Petrol.* **2004**, *80*, 173. [[CrossRef](#)]
81. Maeda, M.; Tomeoka, K.; Seto, Y. Early aqueous alteration process in the QUE97990 and Y791198 CM carbonaceous chondrites. *J. Miner. Pet. Sci.* **2009**, *104*, 92–96. [[CrossRef](#)]
82. Zhou, W.; Peacor, D.R.; Alt, J.C.; Van der Voo, R.; Kao, L.-S. TEM study of the alteration of interstitial glass in MORB by inorganic processes. *Chem. Geol.* **2001**, *174*, 365–376. [[CrossRef](#)]
83. Bouquain, S.; Arndt, N.T.; Hellebrand, E.; Faure, F. Crystallochemistry and origin of pyroxenes in komatiites. *Contrib. Miner. Pet.* **2009**, *158*, 599–617. [[CrossRef](#)]
84. Shore, M.; Fowler, A.D. The origin of spinifex texture in komatiites. *Nature* **1999**, *397*, 691–694. [[CrossRef](#)]
85. Rietmeijer, F.J.; Nuth, J.A.; Rochette, P.; Marfaing, J.; Pun, A.; Karner, J.M. Deep metastable eutectic condensation in Al-Fe-SiO₂-H₂-O₂ vapors: Implications for natural Fe-aluminosilicates. *Am. Miner.* **2006**, *91*, 1688–1698. [[CrossRef](#)]
86. Chizmadia, L.J.; Brearley, A.J. Mineralogy, aqueous alteration, and primitive textural characteristics of fine-grained rims in the Y-791198 CM2 carbonaceous chondrite: TEM observations and comparison to ALHA81002. *Geochim. Cosmochim. Acta* **2008**, *72*, 602–625. [[CrossRef](#)]
87. Zanetta, P.-M.; Leroux, H.; Le Guillou, C.; Zanda, B.; Hewins, R. Nebular thermal processing of accretionary fine-grained rims in the Paris CM chondrite. *Geochim. Cosmochim. Acta* **2020**, *295*, 135–154. [[CrossRef](#)]

88. Haenecour, P.; Floss, C.; Zega, T.J.; Croat, T.K.; Wang, A.; Jolliff, B.L.; Carpenter, P. Presolar silicates in the matrix and fine-grained rims around chondrules in primitive CO3.0 chondrites: Evidence for pre-accretionary aqueous alteration of the rims in the solar nebula. *Geochim. Cosmochim. Acta* **2018**, *221*, 379–405. [[CrossRef](#)]
89. Leitner, J.; Vollmer, C.; Floss, C.; Zipfel, J.; Hoppe, P. Ancient stardust in fine-grained chondrule dust rims from carbonaceous chondrites. *Earth Planet. Sci. Lett.* **2016**, *434*, 117–128. [[CrossRef](#)]
90. Sears, D.W.G.; Benoit, P.H.; Jie, L. Two chondrule groups each with distinctive rims in Murchison recognized by cathodoluminescence. *Meteoritics* **1993**, *28*, 669–675. [[CrossRef](#)]
91. Takayama, A.; Tomeoka, K. Fine-grained rims surrounding chondrules in the Tagish Lake carbonaceous chondrite: Verification of their formation through parent-body processes. *Geochim. Cosmochim. Acta* **2012**, *98*, 1–18. [[CrossRef](#)]
92. Tomeoka, K.; Ohnishi, I. Olivine-rich rims surrounding chondrules in the Mokoia CV3 carbonaceous chondrite: Further evidence for parent-body processes. *Geochim. Cosmochim. Acta* **2014**, *137*, 18–34. [[CrossRef](#)]
93. Metzler, K.; Bischoff, A.; Stöffler, D. Accretionary dust mantles in CM chondrites: Evidence for solar nebula processes. *Geochim. Cosmochim. Acta* **1992**, *56*, 2873–2897. [[CrossRef](#)]
94. Lauretta, D.S.; Hua, X.; Buseck, P.R. Mineralogy of fine-grained rims in the alh 81002 cm chondrite. *Geochim. Cosmochim. Acta* **2000**, *64*, 3263–3273. [[CrossRef](#)]
95. Zolensky, M.; Barrett, R.; Browning, L. Mineralogy and composition of matrix and chondrule rims in carbonaceous chondrites. *Geochim. Cosmochim. Acta* **1993**, *57*, 3123–3148. [[CrossRef](#)]
96. Tomeoka, K.; Tanimura, I. Phyllosilicate-rich chondrule rims in the vigarano cv3 chondrite: Evidence for parent-body processes. *Geochim. Cosmochim. Acta* **2000**, *64*, 1971–1988. [[CrossRef](#)]
97. Hanowski, N.P.; Brearley, A.J. Aqueous alteration of chondrules in the CM carbonaceous chondrite, Allan Hills 81002: Implications for parent body alteration. *Geochim. Cosmochim. Acta* **2001**, *65*, 495–518. [[CrossRef](#)]
98. Lauretta, D.S.; Buseck, P.R. Opaque Minerals in Chondrules and Fine-Grained Chondrule Rims in the Bishunpur (LL3. 1) Chondrite. *Meteorit. Planet. Sci.* **2003**, *38*, 59–79. [[CrossRef](#)]
99. Alexander, C. Trace element contents of chondrule rims and interchondrule matrix in ordinary chondrites. *Geochim. Cosmochim. Acta* **1995**, *59*, 3247–3266. [[CrossRef](#)]
100. Noguchi, T.; Nakamura, T.; Nozaki, W. Mineralogy of phyllosilicate-rich micrometeorites and comparison with Tagish Lake and Sayama meteorites. *Earth Planet. Sci. Lett.* **2002**, *202*, 229–246. [[CrossRef](#)]
101. Graham, G.A.; Bradley, J.P.; Bernas, M.; Stroud, R.M.; Dai, Z.R.; Floss, C.; Stadermann, F.J.; Snead, C.J.; Westphal, A.J. *Focused Ion Beam Recovery and Analysis of Interplanetary Dust Particles (IDPs) and Stardust Analogues. Lunar and Planetary Science XXXV: Interplanetary Dust and Aerogel*; NASA: Washington, DC, USA, 2004.
102. Morris, M.A.; Desch, S.J. Phyllosilicate Emission from Protoplanetary Disks: Is the Indirect Detection of Extrasolar Water Possible? *Astrobiology* **2009**, *9*, 965–978. [[CrossRef](#)] [[PubMed](#)]
103. Deloule, E.; Robert, F. Interstellar Water in Meteorites? *Geochim. Cosmochim. Acta* **1995**, *59*, 4695–4706. [[CrossRef](#)] [[PubMed](#)]
104. Richard A. Catlow, C.; Helen, E. Where on Earth Has Our Water Come From? *Chem. Commun.* **2010**, *46*, 8923–8925.
105. Wasson, J.T.; Rubin, A.E. Composition of matrix in the CR chondrite LAP 02342. *Geochim. Cosmochim. Acta* **2009**, *73*, 1436–1460. [[CrossRef](#)]
106. Cohen, B.A.; Hewins, R.H.; Alexander, C.M. The formation of chondrules by open-system melting of nebular condensates 1 Associate editor: C. Koerberl. *Geochim. Cosmochim. Acta* **2004**, *68*, 1661–1675. [[CrossRef](#)]
107. Rubin, A.E.; Wasson, J.T. Non-Spherical Lobate Chondrules in CO3. 0 Y-81020: General Implications for the Formation of Low-FeO Porphyritic Chondrules in CO Chondrites. *Geochim. Cosmochim. Acta* **2005**, *69*, 211–220. [[CrossRef](#)]
108. Ivanov, D.S.; Zhigilei, L.V. Effect of Pressure Relaxation on the Mechanisms of Short-Pulse Laser Melting. *Phys. Rev. Lett.* **2003**, *91*, 105701. [[CrossRef](#)]
109. Ivanov, D.S.; Zhigilei, L.V. Kinetic Limit of Heterogeneous Melting in Metals. *Phys. Rev. Lett.* **2007**, *98*, 195701. [[CrossRef](#)]
110. Auxerre, M.; Faure, F.; Lequin, D. The effects of superheating and cooling rate on olivine growth in chondritic liquid. *Meteorit. Planet. Sci.* **2022**, *57*, 1474–1495. [[CrossRef](#)]

Disclaimer/Publisher’s Note: The statements, opinions and data contained in all publications are solely those of the individual author(s) and contributor(s) and not of MDPI and/or the editor(s). MDPI and/or the editor(s) disclaim responsibility for any injury to people or property resulting from any ideas, methods, instructions or products referred to in the content.